

Genetic architecture, biochemical underpinnings and ecological impact of floral UV patterning

MARCUS T. BROCK,* LAUREN K. LUCAS,† NICKOLAS A. ANDERSON,‡ MATTHEW J. RUBIN,* R. J. CODY MARKELZ,§ MICHAEL F. COVINGTON,§ UPENDRA K. DEVISETTY,§ CLINT CHAPPLE,‡ JULIN N. MALOOF§ and CYNTHIA WEINIG*¶

*Department of Botany, University of Wyoming, Laramie, WY 82071, USA, †Department of Biology, Utah State University, Logan, UT 84322, USA, ‡Department of Biochemistry, Purdue University, West Lafayette, IN 47907, USA, §Department of Plant Biology, University of California, Davis, CA 95616, USA, ¶Department of Molecular Biology, University of Wyoming, Laramie, WY 82071, USA

Abstract

Floral attraction traits can significantly affect pollinator visitation patterns, but adaptive evolution of these traits may be constrained by correlations with other traits. In some cases, molecular pathways contributing to floral attraction are well characterized, offering the opportunity to explore loci potentially underlying variation among individuals. Here, we quantify the range of variation in floral UV patterning (i.e. UV 'bull's-eye nectar guides) among crop and wild accessions of *Brassica rapa*. We then use experimental crosses to examine the genetic architecture, candidate loci and biochemical underpinnings of this patterning as well as phenotypic manipulations to test the ecological impact. We find qualitative variation in UV patterning between wild (commonly lacking UV patterns) and crop (commonly exhibiting UV patterns) accessions. Similar to the majority of crops, recombinant inbred lines (RILs) derived from an oilseed crop × WI fast-plant[®] cross exhibit UV patterns, the size of which varies extensively among genotypes. In RILs, we further observe strong statistical-genetic and QTL correlations within petal morphological traits and within measurements of petal UV patterning; however, correlations between morphology and UV patterning are weak or nonsignificant, suggesting that UV patterning is regulated and may evolve independently of overall petal size. HPLC analyses reveal a high concentration of sinapoyl glucose in UV-absorbing petal regions, which, in concert with physical locations of UV-trait QTLs, suggest a regulatory and structural gene as candidates underlying observed quantitative variation. Finally, insects prefer flowers with UV bulls-eye patterns over those that lack patterns, validating the importance of UV patterning in pollen-limited populations of *B. rapa*.

Keywords: *Brassica rapa*, nectar guide, pollinator behaviour, sinapate ester, UV pattern

Received 17 June 2015; revision received 17 December 2015; accepted 22 December 2015

Introduction

Diverse visual attraction traits have been identified as critical to reproductive success and in maintaining species boundaries for both plants and animals (Jones & Hunter 1993; Domb & Pagel 2001; Bradshaw & Schemske 2003). In plants, variation in floral size (e.g.

corolla size; Galen 1996; Glaetli & Barrett 2008), shape and symmetry (Møller 1995), and colour (Bradshaw & Schemske 2003; Hoballah *et al.* 2007) has been shown to enhance the frequency and quality of pollinator visitation. Similarly, floral patterning (e.g. nectar guides, converging lines, spots or bulls-eye regions), which is prevalent in angiosperm corollas (Penny 1983; Dyer 1996), can enhance pollinator attraction (Johnson & Midgley 1997) and has been shown to increase the frequency of effective pollinator visits by reducing

Correspondence: Marcus T. Brock, Fax: +1 307 766 2851; E-mail: mbrock2@uwyo.edu

handling times (Waser & Price 1985; Leonard & Papaj 2011; Hansen *et al.* 2012; Leonard *et al.* 2013). Like other quantitative traits, the evolution of attraction traits depends on the magnitude of segregating genetic variation as well as on the strength of genetic covariation among attraction traits and other aspects of floral morphology. If the major axis of trait covariation is parallel to the joint vector of selection, then evolutionary responses may be enhanced, whereas responses may be slowed if trait covariation is antagonistic to the vector of selection (Schluter 1996; Etersson & Shaw 2001). To explore evolutionary constraints, it is valuable to characterize the statistical-genetic and quantitative trait loci (QTL) architecture. By relating genetic maps to physical ones, QTL screens that identify genomic regions affecting a trait (or multiple traits) can inform bioinformatic analyses of functionally annotated positional candidates that may contribute to or constrain adaptive evolution.

The biochemistry of many visual attraction traits is well characterized in plants, which has enabled elegant studies of the evolution of floral colour and patterning and an understanding of the molecular genetics underlying these pollinator attraction phenotypes (reviewed in Sobel & Streisfeld 2013; Yuan *et al.* 2013a). For example, the flavonoid branch of the phenylpropanoid pathway is responsible for the production of red, purple and blue anthocyanin pigments (Holton & Cornish 1995). Examination of genes regulating floral colour reveals highly conserved regulatory mechanisms for this biochemical pathway. R2R3-MYB transcription factors (Stracke *et al.* 2001) in concert with their interacting WD40 and bHLH protein partners (Walker *et al.* 1999; Heim *et al.* 2003; Ramsay & Glover 2005) are key regulators of both floral anthocyanin production and pigment patterning in a variety of distantly related angiosperms (deVetten *et al.* 1997; Walker *et al.* 1999; Carey *et al.* 2004; Pang *et al.* 2009; Pattanaik *et al.* 2010). Discrete differences in floral colour (Bradshaw & Schemske 2003; Hoballah *et al.* 2007) as well as more subtle intraspecific variation in anthocyanic nectar guides (Medel *et al.* 2003; Shang *et al.* 2011) have been shown to influence the species specificity of pollinator visitation. In addition to anthocyanins, variation in UV-absorbing flavonoids (Thompson *et al.* 1972; Dement & Raven 1974; Gronquist *et al.* 2001; Sasaki & Takahashi 2002; Matsubara *et al.* 2012) is responsible for nectar guide patterns in the near-ultraviolet region of the solar spectrum (~350 nm), and these UV patterns are perceived by most flower-visiting insects (Briscoe & Chittka 2001). The phenylpropanoid pathways contributing to the production of UV-absorbing compounds are well characterized (Buer *et al.* 2010; Milkowski & Strack 2010; Vogt 2010), suggesting candidate loci that may contribute to UV patterning in flowers.

Floral nectar guides and pigments in the UV spectrum are no more, or less, important to pollinator behaviour than those in the human-visible spectrum that are also perceived by insects (Kevan *et al.* 2001). Yet, these more cryptic UV phenotypes have received somewhat less attention. From a distance, pollinators identify and choose flowers using a variety of traits including their size and visual contrast relative to the background (i.e. contrast perceived by their green photoreceptors), both of which influence floral apparency (Spaethe *et al.* 2001). At closer proximity to flowers, bees have been shown to initially approach petal margins and, when present, utilize bulls-eye patterns to more rapidly direct their approach and identify floral rewards (Lunau 1990; Lunau *et al.* 2006). Broad surveys of angiosperms indicate that petal margin and nectar guides predominantly have complementary symmetries (i.e. flowers and their nectar guides are both either radially symmetrical or bilaterally symmetrical) (Dafni & Kevan 1996), which may facilitate foraging efficiency. Correlations in the symmetry of different floral features may arise from pollinator selection (and resulting linkage disequilibrium) or arise from a common genetic developmental programme (i.e. pleiotropy). Floral attraction traits have been studied using artificial model flowers to experimentally manipulate attraction traits and test for visitor behavioural responses (e.g. Lunau *et al.* 2006; Leonard & Papaj 2011). UV patterning is likewise amenable to phenotypic engineering via application of UV-absorbing pigments to corollas (Johnson & Andersson 2002), allowing for experimental tests of the influence of nectar guides on foraging insect behaviour (Koski & Ashman 2014).

Here, we first examine UV patterning in wild vs. crop populations of *Brassica rapa* and then characterize the quantitative-genetic and QTL architecture as well as positional candidates for UV patterning in recombinant inbred lines (RILs). We further quantify, via HPLC and GC-MS, compounds contributing to this patterning in addition to effects of floral patterning on pollinator behaviours. Specifically, we address the following questions: (i) Is selection history (natural vs. artificial) associated with the presence vs. absence of UV patterning, and how does the range of patterns observed in crop and wild accessions compare with that in RILs? (ii) What is the quantitative-genetic and QTL architecture of size and shape components of petal blades and petal UV region in RILs? Specifically, what is the degree of correlation within and between petal blade and UV patterning traits? (iii) From QTL mapping and localization on the physical map, do genomic regions affecting UV patterning suggest candidate genes that might regulate UV pigment production? (iv) Do concentrations of UV-absorbing

phenylpropanoid compounds covary with UV patterning in petal tissue regions? (v) Does experimental manipulation of the presence vs. absence of UV patterns influence insect visitation under field conditions, and how do floral UV phenotypes of crop and wild accessions compare to those favoured by insects?

Materials and methods

Brassica rapa (Brassicaceae) is native to temperate regions of Western Europe and Asia. As a consequence of crop diversification and numerous introductions, *B. rapa* is now present as both a weed and crop on all inhabited continents (Holm *et al.* 1997). Human selection has generated a number of crop varieties, which are globally cultivated as leaf vegetables (subsp. *chinensis* and *pekinensis*), root vegetables (subsp. *rapa*) and oilseeds (subsp. *oleifera*). *B. rapa* plants produce a racemose inflorescence with archetypal brassicaceous flowers containing four whorls: four sepals, four yellow petals, six stamens (two short and four long) and a compound pistil. Although this species commonly relies on insect visitors to deposit outcrossed pollen due to sporophytic self-incompatibility (Bateman 1955), self-compatibility has evolved in both wild populations and crop accessions (Nou *et al.* 1993; Zhao *et al.* 2005).

Flowers of *B. rapa* have pronounced differences in size and symmetry (Fig. 1A–C). Flowers of two varieties (subsp. *pekinensis* and subsp. *rapa*) have previously been shown to have UV bulls-eye patterns (Sasaki & Takahashi 2002; Yoshioka *et al.* 2005), and HPLC analyses of subsp. *pekinensis* support a UV-absorbing flavonoid compound, isorhamnetin 3,7-*O*-di- β -D-glucopyranoside, as the source of the UV-absorbing region of the bulls-eye pattern (Sasaki & Takahashi 2002). We first surveyed wild and crop accessions to describe variation in UV patterning in *B. rapa*. This survey provides a basis for understanding the species relative to RIL variation in floral UV patterns, that is the variation that arises in part from past artificial or natural selection vs. from segregating variation between the parents of our cross, respectively. The accession survey also provides a useful reference for the phenotypic manipulation experiment and reveals whether floral UV phenotypes observed in crop or wild genotypes are consistent with pollinator-mediated selection.

We utilized RILs and the parental genotypes to examine the statistical-genetic architecture, biochemical underpinnings and insect preference for UV patterning in a segregating progeny. The RIL population was established by crossing two self-compatible genotypes, R500 and IMB211, producing an F1 that was self-pollinated to produce F2 progeny, which were selfed and

propagated through single-seed descent for six generations (Iniguez-Luy *et al.* 2009). R500 is a yellow sarson oilseed variety originating in India, while IMB211 is a derivative of the Wisconsin fast-plant[®] population (Williams & Hill 1986). R500 plants attain larger size and biomass as a consequence of later flowering time relative to IMB211, which matures rapidly as a result of artificial selection. Flowers of these two genotypes differ in the size and shape of the UV pattern (cf Fig. 1E vs. F, see Results).

Population-level survey of UV patterning

To explore variation in the presence vs. absence of UV patterning in *B. rapa*, we raised both wild and crop accessions in agricultural fields (summers 2010 and 2012) at the Agricultural Experiment Station at the University of Wyoming (UW-AES; Laramie, WY, USA). In total across both years, we imaged flowers from six wild populations of *B. rapa* from California, USA, and 15 crop accessions from six subspecies of *B. rapa* obtained from germplasm centres (www.ars-grin.gov; www.wageningenur.nl). In early June of each year, we raised a minimum of six replicates per accession in the UW-AES greenhouses; we planted three seeds per accession in peat pots (9 cm square \times 10 cm tall; 350 cm³) containing soil from the adjacent field sites where the plants were ultimately transplanted. Pots were supplemented with ~2.2 g of Osmocote 18–6–12 slow-release fertilizer (Scotts Miracle Grow, Marysville, OH, USA) and watered daily. Greenhouse temperatures were regulated to match ambient outside temperatures with a minimum threshold of 8 °C at night.

One week after germination, pots were thinned to one seedling, and 1 week later, we transplanted pots into the nearby UW-AES fields. Pots were planted into a randomized block design with one replicate of each accession per block with a minimum of 25 cm between adjacent plants. Experimental plants were watered twice daily (0430 and 1800) via a permanent sprinkler irrigation system. Plants were monitored daily for flowering and the appearance of both reflexed petals and dehiscent anthers, at which point we harvested a newly opened flower between 0900 and 1200 h. Flowers were transported to the laboratory and imaged in the UV spectrum. Digital photographs were recorded using a full spectrum digital camera sensitive to UV wavelengths (Life Pixel, Mukilteo, WA, USA) coupled to a UV lens and filter (Baader Planetarium, Mammendorf, Germany) that together restricted wavelengths to 350–400 nm. Flowers were illuminated with standard blacklight-blue bulbs that produce wavelengths at ~365 nm.

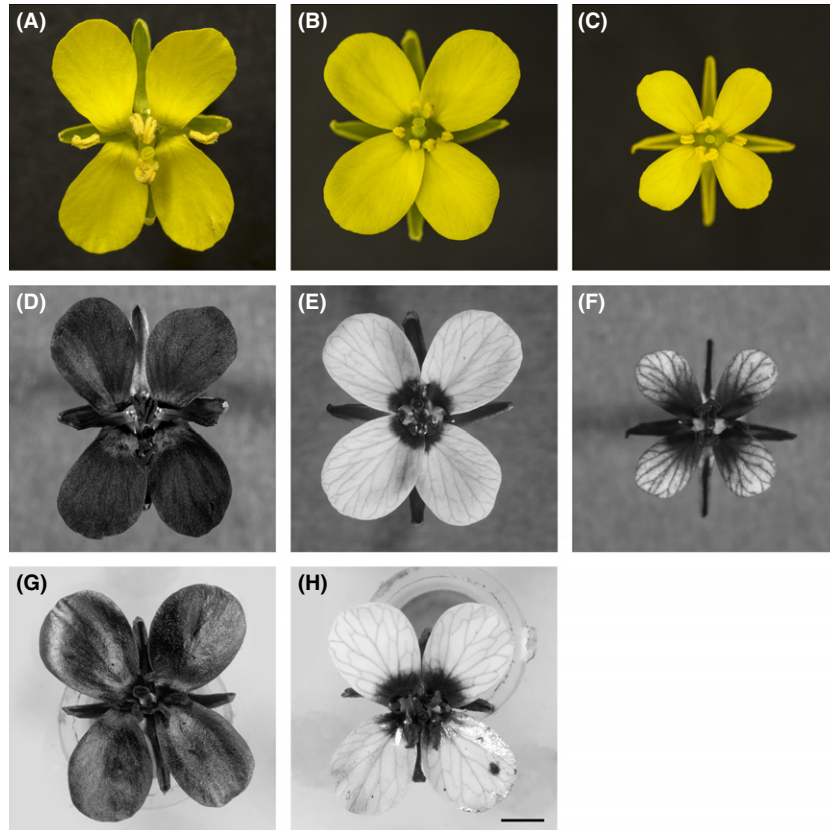


Fig. 1 Visible spectrum (A–C) and UV (~360 nm; D–F) photographs of *Brassica rapa* flowers. (A, D) Patternless UV phenotype found in weedy populations and some crop accessions (see Table 1; imaged flower from a weedy accession, Newport Harbor, CA, USA); (B, E and C, F) UV bulls-eye-patterned flowers and the range of variation in proportion UV (UVP) found in *B. rapa* RILs (imaged flowers from RIL 357 and parental IMB211 genotypes, respectively). (G) A UV-patterned flower painted with sunscreen dissolved in duck fat. (H) A UV-patterned flower with lower petals painted with duck fat (upper petals were not manipulated for comparison; imaged flower from RIL 31, inclusive scale bar = 2.5 mm).

Survey of *Brassica rapa* herbarium specimens

Given variation in the presence vs. absence of UV bulls-eye patterns in field-grown wild populations and crop accessions (see Results), we expanded our survey to include herbarium sheets ($N = 32$) available in the Rocky Mountain Herbarium at the University of Wyoming (Laramie, WY, USA). We imaged herbarium sheets in the UV spectrum as described above and were able to visualize the presence of UV bulls-eye patterns from samples collected throughout North American and Scandinavian countries as early as 1898. Samples that lacked distinct bulls-eye patterns were classified as patternless, UV-absorbing flowers. Given that UV patterns were observed in flowers of *B. rapa* collected 117 years ago, results of this survey assume that UV-absorbing/UV-reflecting petal compounds in this species are stable over time and that variation in herbarium sample preparation does not influence qualitative variation (presence vs. absence) in UV patterns. Herbarium sheets that had been subjected to mercury chloride treatment

were glossy in comparison with other herbarium samples; we excluded these samples from the survey.

Quantitative-genetic examination of UV patterning in RILs

We measured morphometric floral data from *B. rapa* RILs raised in the UW-AES fields. Plants in this experiment were part of a larger quantitative-genetic experiment exploring the effects of crowding and drought on plant performance and physiology. Here, we describe floral data measured from six replicate plants raised in a low-density well-watered growth environment.

Similar to the field surveys above, we planted seeds of each of 125 RILs and the two parental lines in the UW-AES greenhouses and following 2 weeks of establishment and growth, seedlings were transplanted into the field. On 8 and 9 June 2010, three seeds of each RIL were planted into each of six replicate pots (three replicates per genotype per day) that were randomized

across six spatial blocks. Pot preparation, greenhouse conditions and transplanting followed the procedures described above for the UV survey experiment.

Plants were monitored daily for date of first flowering and 2 days later a newly opened flower was collected from each plant between 0900 and 1200 h. One representative petal from each flower was removed and flattened on double-sided tape to reveal the adaxial petal surface (i.e. the side visible to approaching insects). Petals were imaged in the UV spectrum as described above. Using IMAGEJ software (vs.1.44; Wayne Rasband; National Institutes of Health, Bethesda, MD, USA), we measured the length of the petal blade (from the distal tip of the petal to the point at which the blade reflexes, i.e. the transition point between petal claw and petal blade), the maximum width of the petal blade and the petal blade area. Similarly, we measured the length, maximum width and area of the UV-absorbing region on the petal blade. We further estimated proportion UV (UVP) as the proportion of the blade area that absorbed UV wavelengths. To estimate the shape of the petal blade and UV pattern, we calculated length-to-width ratios (L/W) of each region; ratios that are closer to one indicate more circular blades.

Flowers (minus the petal removed above) were then preserved in 70% ethanol. Later, flowers were dissected and imaged under a stereomicroscope (Nikon SMZ-800, Tokyo, Japan). In IMAGEJ, we measured the length of each of the following floral organs: sepal, long stamen, short stamen and pistil.

Statistical methods

We used ANOVA (PROC MIXED, SAS 9.2) to partition variation in petal and UV region sizes and shapes between two random factors: RIL genotype and spatial block. We also extracted principal components (PC; PROC PRINCOMP, SAS 9.2) of floral organ size as estimated with the length of the following traits: sepal, long stamen, short stamen and pistil. We retained the first PC as our metric of floral size, which explained 71.8% of the variation (Table S1, Supporting information). To improve normality, L/W ratios of petal blade and UV-pattern region were log-transformed, UVP was arcsine-transformed, and all other traits were Box-Cox-transformed (Box & Cox 1964; Sokal & Rohlf 1995). Using genotype, block and residual variance components resulting from these mixed models, we estimated broad-sense heritability (H^2 ; V_G/V_P) for all petal, UV pattern and PC traits (Falconer & Mackay 1996).

Back-transformed genotypic values of each RIL (best linear unbiased predictors, BLUPs; PROC MIXED, SAS 9.2) were subsequently used to explore the statistical-genetic and QTL architecture by estimating bivariate

correlations (i.e. genetic correlations; PROC CORR, SAS 9.2) and by testing for main-effect and epistatic QTL (see Linkage map construction and QTL analyses). Genetic correlation *P*-values were Bonferroni corrected to account for multiple comparisons (Sokal & Rohlf 1995).

Analytical characterization of phenylpropanoid compounds underlying UV patterning

To identify the secondary compounds underlying the petal UV patterning present in the RIL population, we used HPLC to separate methanolic soluble extracts from UV-absorbing (petal blade base) and UV-reflecting (petal blade tip) petal regions. We focused on peaks with appreciable differences in peak area (i.e. concentration) across these tissue regions. Initial HPLC analyses were performed on flowers from a single replicate of R500 raised in the UW-AES fields in the summer of 2011 (planting methods described above). Petal blades of R500 were dissected into UV-absorbing and UV-reflecting tissue regions using the 'live view' function of our modified UV digital camera. Each tissue region was placed in a microcentrifuge tube with 50% methanol (0.01 mg fresh tissue/100 μ L of solvent) and incubated for 1 h at 60 °C. Methanolic soluble extractions were stored at -80 °C and analysed via HPLC on a Shim-pack XR-ODS column (3.0 \times 75 mm, 2.2 μ m; Shimadzu, Kyoto, Japan) as previously described (Fraser *et al.* 2007).

We selected two peaks as candidates for further characterization and identification (peaks 3 and 4; Fig. S1, Supporting information), because they absorbed UV wavelengths visible to UV-sensitive insects (~350 nm). Methanol extractions of UV-absorbing and UV-reflecting petal regions of R500 were analysed using LC-MS (Agilent 1200 HPLC system coupled with an Agilent 6460 triple-quadrupole MS, utilizing positive mode Jet-Stream ESI, Palo Alto, CA, USA) as previously described (Lee *et al.* 2012). We focused our analyses on compounds consistent with either isorhamnetin (isorhamnetin 3,7-*O*-di- β -D-glucopyranoside), which was previously reported as underlying the *B. rapa* UV patterning (Sasaki & Takahashi 2002), or sinapoyl glucose (1-*O*-sinapoyl- β -glucose), which was suggested by the fluorescence profile of peak 3 emitting 420 nm when excited by 330 nm wavelengths (Li *et al.* 2010). In addition, the retention time of peak 3 was found to be the same as the retention time of the peak corresponding to sinapoyl glucose, which accumulates in the *sinapoylglucose accumulator1 Arabidopsis* mutant (data not shown) (Li *et al.* 2010).

We quantified the concentration of peaks 3 and 4 in UV-absorbing and UV-reflecting petal regions to

determine whether they covaried with floral UV patterning. We dissected petal blades into UV-absorbing and UV-reflecting regions from four replicates each of R500 and IMB211 growing in the UW-AES fields in 2011 and extracted phenylpropanoids. We used sinapic acid to quantify concentrations of peak 3 (sinapoyl glucose; see Results) and quercetin for peak 4 (isorhamnetin; see Results), because those are the UV-absorbent moieties on each compound, respectively. Using ANOVA, we partitioned variance in concentration of each compound among the following fixed factors: genotype, tissue region and the genotype \times tissue region interaction (PROC MIXED, SAS 9.2).

QTL analyses

We used composite interval mapping (CIM; WinQTL-Cart vs. 2.5; Wang *et al.* 2007), to explore the QTL architecture of floral, petal, and UV region size and shape traits. Using a preliminary linkage map of 1273 SNPs across the ten *B. rapa* chromosomes (M.F. Covington, R.J.C. Markelz, U.K. Devisetty, M.T. Brock, M.J. Rubin, C. Weinig & J.N. Maloof, in preparation; see Data S1, Supporting information for details of linkage map construction), we tested for QTL at least every cM, using a window size of 10 cM to prevent proximally confounding covariates from entering the model. We calculated significant (P -value < 0.05) and marginally significant (P -value < 0.075) genomewide thresholds by permuting the data set 1000 times for each trait (Churchill & Doerge 1994). All QTL analyses were performed on RIL genotypic values (BLUPs; see Morphological Statistical methods).

We further tested for effects of epistatic interactions on all measured traits using R/QTL *scantwo* analyses (Broman *et al.* 2003), which tests all possible marker \times marker combinations for their interactive effect on floral traits. For these analyses, we implemented the maximum-likelihood algorithm with a window size of 10 cM. To determine significance of each interaction, we estimated a genomewide threshold by permuting the data set 1000 times.

To identify possible candidate genes regulating UV patterning, we selected three QTL with narrow 2-LOD support limits that regulate multiple UV region size traits (QTL3-3, QTL7-3 and QTL8-2; see Results). We extracted *Brassica* genes within each 2-LOD interval from the *B. rapa* reference genome (v1.5; www.brassicadb.org) and for each determined the best *Arabidopsis thaliana* homologous gene (or 'best hit' via the BLASTx algorithm; Altschul *et al.* 1997). We screened both chromosomal regions for homologs to known *Arabidopsis* genes in the phenylpropanoid pathway as well as regulatory genes in MYB, bHLH, WD and UDP-glycosyl-

transferase families, which have been shown to regulate production of phenylpropanoids (Hemm *et al.* 2001; and citations from the introduction). We utilized the NetworkDrawer web-based analysis tools of ATTED-II and the associated database of gene co-expression patterns (<http://atted.jp/>; Obayashi *et al.* 2011) to examine whether candidates underlying identified UV-trait QTL are co-expressed with genes known from phenylpropanoid pathways. Finally, utilizing RNA-Seq data from the R500 \times IMB211 RIL population (Devisetty *et al.* 2014), we examined the coding sequence of candidate genes emerging from analyses above to determine (i) whether amino acid structure differs across parental alleles and (ii) whether these possible amino acid substitutions potentially influence protein function based on differences in physicochemical properties (Blossum80 substitution matrix; Henikoff & Henikoff 1992) or proximity to putative functional domains.

Effects of UV patterning on insect visitation

In July 2011 field trials, we monitored insect visitation to plants with flowers that had either a UV bulls-eye pattern or lacked a pattern (UV-absorbing flowers; Fig. 1). Patternless/UV-absorbing flowers were generated by applying sunscreen dissolved in duck fat to petal blades (Johnson & Andersson 2002). This experimental technique modifies reflectance of UV wavelengths; however, the duck fat does not alter the spectral profile of visible wavelengths of light (400–700 nm). Replicate plants of the *B. rapa* R500 genotype, which has a bulls-eye UV pattern, were randomly assigned to one of three treatments: an internal control (C; flowers not manipulated), a bulls-eye control (UV+; petal blades were painted with duck fat) or a nonpatterned/UV-absorbing treatment (UV–; petal blades were painted with sunscreen dissolved in duck fat).

We planted 60 replicates of R500 in early June of 2011 as previously described. Plants were thinned in the greenhouse and transplanted into 20 spatial blocks in the UW-AES fields in mid-June. In the mornings (0900 MST) between 26 and 29 July 2011, UV treatments were randomly assigned to three replicate R500 plants in each of 3–10 spatial blocks (depending on the day). We applied duck fat or duck fat plus sunscreen to petal blades of the newly opened flowers of plants assigned to UV+ and UV– treatments, respectively. Between 1000–1200 MST, all insect visits to plants in each block were recorded for 30-min intervals. Up to five assistants sat and observed insect visitation, resulting in a total of 36 independent observation periods. For each insect visitor, we recorded the sequence of experimental plants visited and how many flowers were landed upon per plant.

Insects were classified based on order-level pollinator guilds of diptera and hymenoptera, with the exception of *Megachilidae* sp., an easily discernable and frequently visiting family, which were catalogued as megachilids. We counted all open flowers per experimental plant per day and removed open flowers at the end of each day to ensure treatment fidelity following randomization the next day.

Insect visitation statistical methods

We conducted mixed-model ANOVA to partition variation in insect visitation among the fixed effects of pollinator guild, UV treatment and the pollinator guild \times UV treatment interaction, and the random effects of date and block nested within date. We included the total number of open flowers per plant as a covariate in our statistical model to control for variation in visitation attributable to display size. We analysed two metrics of insect visitation; first, the total number of insect visits to experimental plants – where repeat visits by the same insect were also counted upon a return from a different plant in the array. Second, we examined variation in the total number of flowers visited per plant by pollinator guilds in the 30-min period. To improve normality, we square-root-transformed visitation counts for both insect visitation metrics. Because dipterans only accounted for 7.7% ($N = 19$) of the visiting insects, we dropped this guild due to low sample size and report analyses of megachilids ($N = 118$) and remaining hymenopterans ($N = 110$).

Results

Population-level and quantitative-genetic variation

At the population level, floral surveys of crop and wild accessions of *Brassica rapa* demonstrate qualitative variation in UV patterning (Fig. 1; Table 1). Most crops (including accessions of broccoletto, komatsuna, pak choi, turnip and oilseed) exhibit a UV bulls-eye pattern; however, 3 (one broccoletto and two oilseed) of the 15 crop accessions examined lack a UV pattern, absorbing UV wavelengths across the entire petal blade. The six wild populations cultivated from seeds collected in California, USA (approximate mean interpopulation distance = 41 km, range = 8–78), had patternless UV-absorbing petal blades; herbarium sheets from 13 different states within the USA also suggest that patternless UV-absorbing flowers may be common among wild populations in North America (Table 1; accession details Table S2, Supporting information). Notably, these North American wild plants resemble oilseed or broccoletto crop types with regard to vegetative morphology (which is very distinct from the high leaf and root allocation typical of cabbage and turnip types, respectively) and with regard to life history (because they lack the vernalization requirement common to vegetable crops), suggesting that North American wild populations originated as volunteers from an unpatterned variant of these crops. Specimens collected across Scandinavia were typically patterned (Table 1; accession details Table S2, Supporting information).

Table 1 Summary counts from a population-level survey of *Brassica rapa* plants producing flowers that are either UV-patterned or lacking a pattern (UV absorbing across the entire petal blade). Plants were raised in the UW-AES fields or are from a survey of specimens available in the Rocky Mountain Herbarium at the University of Wyoming. Bold font denotes the presence of at least one dark/patternless sample from a specific origin locality. Detailed information on each sample is listed in Table S2, Supporting information

Group	Sampling method	Samples	Origin	UV patterned	Dark/patternless	Total Sample Number
Wild	Field	Six populations (USA)	CA	0	6	6
Wild	Herbarium	North America (12 USA states)	AK, CA, FL, ID, KS, LA, MA, MI, MT, NE, NJ, UT, WY	6	21	27
Wild	Herbarium	Scandinavia (three countries)	Denmark, Finland, Sweden	5	0	5
Broccoletto	Field	Two accessions	Italy , Japan	1	1	2
Komatsuna	Field	One accession	Japan	1	0	1
Pak choi	Field	One accession	China	1	0	1
Turnip	Field	Two accessions	Japan	2	0	2
Oilseed	Field	Nine accessions	Canada , Egypt, Germany, India, Pakistan, Sweden	7	2	9

All RILs in our segregating progeny have UV bulls-eye patterns, and the population expresses significant quantitative variation in all measured aspects of petal blade and UV region size (area, length and width) and allometry (L/W ratio, UVP; Table 2). Additionally, the first principal component axis of the length of sepal, long stamen, short stamen and pistil explained 71.8% of the size variation in these traits (Table S1, Supporting information) and ANOVA of this floral size PC indicates significant genetic variation segregating in the *B. rapa* RIL population (Table 2). The range of genotypic means for all traits with positive values (i.e. excluding PC1) was extreme, increasing by an average of 3.5-fold (range: 1.6- to 8.3-fold increase). Broad-sense heritability of all traits was also high, averaging 0.49 (range: 0.19–0.67; Table 2).

We detected uniformly strong genetic correlations within size measurements of the petal blade (mean = 0.86) and within size estimates of the UV region (mean = 0.85); however, correlations between traits in these two groups were considerably weaker or nonsignificant (mean = 0.36; Table 3; Fig. S2, Supporting information). Similarly, petal blade area, length and width were highly correlated with the length of other floral whorls (i.e. floral size PC; mean = 0.70), while the UV region size traits were more weakly correlated with the floral size PC (mean = 0.37; Table 3). Strong petal shape–petal width and UV shape–UV length correlations indicate that shape variation (i.e. L/W ratio) in petal blades vs. petal UV patterning is predominantly driven by different morphological axes (i.e. width and length, respectively). Most notably, the proportion of the petal blade that absorbs UV (UVP) was only significantly correlated with aspects of UV region size,

indicating that it is genetically independent of petal blade size and largely controlled by variation in the UV region itself.

QTL mapping

We detected an average of 5.6 main-effect QTL (range = 2–8) for each of the ten floral traits (Fig. 2, Appendix 1; for marker physical positions and support limits, see Table S3, Supporting information). Individually, these QTL explained an average of 8.8% of the genetic variance (range = 3.5–34.5% per cent variance explained; PVE) in floral traits and taken together explain an average of 46.9% (range = 20.5–67.1%) of the genetic variation of each trait. While a majority of the detected QTL were of low/moderate effect size (91% of QTL had effect sizes of <15% PVE), we detected several QTL of major effect; QTL3–5 on A03 contributes 22.0% of the V_g in petal blade width and 34.5% of the variance in petal blade L/W ratio. QTL9-1 and QTL9-3 explain 18.8% and 17.3%, respectively, of the variance in the first axis of the floral size PCA. Inheritance of alleles from R500 typically increased petal blade size traits but had a more variable influence on the size of the UV region, indicating that both R500 and IMB211 contribute positive alleles for size of the petal UV region.

Several genomic regions are ‘hotspots’ controlling variation in multiple floral traits, contributing to observed strong positive correlations within either petal blade or UV region size traits (Table 3; Fig. 2). For example, petal blade size traits are pleiotropically regulated by QTL1-1, 7-1, 9-2 and 9-3, while UV region size traits are predominantly regulated by a distinct suite of pleiotropic QTL – QTL3-3, 7-3, 8-2, 10-2. QTL3-3, 7-3 and 8-2 also regulate the proportion of the petal blade that absorbs UV wavelengths (UVP) and contribute to the strong genetic correlations observed between UV region size and UVP.

We detected 13 QTL × QTL epistatic interactions across measured floral traits. On average, epistatic interactions accounted for 3.2% (range = 1.2–8.5% PVE) of the genetic variance in this population; however, this may be an underestimation of the importance of epistatic interactions because low replication of allelic combinations in multiway interactions reduces power. Two pleiotropic epistatic interactions influence multiple petal size traits, and thus, epistatic interactions also contribute to strong genetic correlations observed for these traits. For example, QTL × QTL interactions between A1 and A10 coregulate UV blade width and UV blade area, while interactions between A4 and A6 influence UV blade length and UVP. This overlapping QTL architecture could partially arise because area and UVP are ultimately derived from base traits such as length and

Table 2 Mixed-model ANOVA of RIL genotype and spatial block on size and shape traits of *Brassica rapa* flowers and petals. Z-values are reported and significance is indicated with asterisks. Broad-sense heritabilities (H^2 ; V_G/V_P) were calculated from estimated variance components of independent variables

Trait	Block	Genotype	H^2
Floral size PC1	1.37	6.46****	0.50
Blade area	1.38	6.81****	0.58
Blade ln	1.24	6.54****	0.52
Blade wd	1.40	6.98****	0.63
Blade L/W ratio	1.33	7.07****	0.67
UV area	1.35	6.45****	0.46
UV ln	1.30	6.67****	0.52
UV wd	1.38	5.63****	0.31
UV L/W ratio	0.77	4.35****	0.19
Proportion UV	1.25	6.56****	0.49

****<0.0001.

Table 3 Genotypic correlations between size and shape traits of flowers, petal blades and petal UV regions of *Brassica rapa* RILs raised in the field at the University of Wyoming. Pearson product-moment correlation coefficients are reported with asterisks indicating significance of the correlation following Bonferroni correction

	Floral size PC1	Blade area	Blade ln	Blade wd	Blade L/W	UV area	UV ln	UV wd	UV L/W	UVP
Floral size PC1	—	0.73****	0.77****	0.61****	-0.08	0.39****	0.31**	0.40****	0.09	0.01
Blade area		—	0.91****	0.94****	-0.40****	0.40****	0.33**	0.46****	0.04	-0.08
Blade ln			—	0.73****	-0.01	0.22	0.18	0.24	0.04	-0.24
Blade wd				—	-0.67****	0.47****	0.40****	0.56****	0.03	0.03
Blade L/W					—	-0.44****	-0.39***	-0.55****	0.00	-0.30**
UV area						—	0.95****	0.87****	0.37***	0.85****
UV ln							—	0.74****	0.57****	0.85****
UV wd								—	-0.03	0.70****
UV L/W									—	0.38***
UVP										—

<0.01; *<0.001; ****<0.0001.

width. However, this explanation seems unlikely given that six of the 13 interactions are unique to a 'composite' trait (e.g. L/W ratio or UVP) and are not identified for underlying length and width traits.

For further bioinformatics analyses, we selected three QTL pleiotropically regulating UV region size traits (QTL3-3; 7-3 and 8-2, Fig. 2; Appendix 1) that have narrow 2-LOD support regions containing 328, 286 and 178 putative *Brassica* genes, respectively. Within these three regions, we detected numerous genes from MYB ($N = 5$), bHLH ($N = 5$), WD40 ($N = 13$) and UDP-dependent glycosyltransferase ($N = 14$) gene families. The majority of these genes are in subfamilies (Li *et al.* 2001; Dubos *et al.* 2010) or are homologous to *Arabidopsis* genes that do not influence sinapate ester or phenylpropanoid production (see Analytical characterization of UV patterning compounds); however, two strong candidates emerged. Under QTL3-3, we identified a gene, Bra000453 (Table S4, Supporting information), homologous to *MYB12* from *Arabidopsis thaliana* (At2g47460), which targets the promoter of a UDP-glucosyltransferase (*UGT84A1*; At4g15480) that catalyses the conversion of sinapic acid to sinapoyl glucose. Under QTL7-3, we identified a homolog (Bra004109; Table S5, Supporting information) of the *Arabidopsis* 4-coumarate:CoA ligase 3 gene (*4CL3*; At1g65060), which is involved in production of early phenylpropanoid precursors to sinapate esters, is a putative target of *MYB12* and is identified in the ATTED-II database as strongly co-expressed with *MYB12* and *UGT84A1*.

Despite a gap of 30 amino acids in IMB211 due to incomplete RNA-Seq coverage, R500 and IMB211 have five nonsynonymous substitutions in Bra000453 (homologous to *MYB12*; for alignment see Fig. S3, Supporting information). Two of these amino acid substitutions

(amino acid 143, G vs. R and amino acid 165, P vs. A) are disfavoured based on amino acid substitution matrices (Blosum80 values: -3 and -1, respectively; where more negative values indicate less favourable substitutions) and are found on either side of the MYB12 subgroup seven motif, which characterizes flavonol transcriptional regulators and may influence binding to *cis*-acting nucleotide sequences (Stracke *et al.* 2001, 2007). Parental genotypes also have eight nonsynonymous substitutions in Bra004109 (homologous to *4CL3*; for alignment see Fig. S4, Supporting information). One substitution (amino acid 212, A vs. V; Blosum80 value = 0) falls within a conserved putative AMP-binding domain (Schneider *et al.* 2003; Sigrist *et al.* 2013) and four additional substitutions are proximal by 18 amino acids.

Analytical characterization of UV patterning compounds

HPLC analyses of R500 petal blades resolved four peaks with differential abundance across absorbing and reflecting petal regions (Fig. S1A, Supporting information). Absorbance profiles of these peaks indicate that only peaks 3 and 4 absorb wavelengths near 360 nm (and would appear darker to insects with UV sensitivity). When excited with 330 nm wavelengths, peak 3 emits 420 nm wavelengths (characteristic of sinapoylated molecules); furthermore, peak 3 co-elutes with a standard of sinapoyl glucose isolated from *Arabidopsis thaliana* leaf extracts (data not shown) (Chapple *et al.* 1992). LC-MS analyses confirmed that peak 3 is sinapoyl glucose (mass 386.1213; chemical formula $C_{17}H_{22}O_{10}$). Absorbance profiles of peak 4 (Fig. S1B, Supporting information) are consistent with an

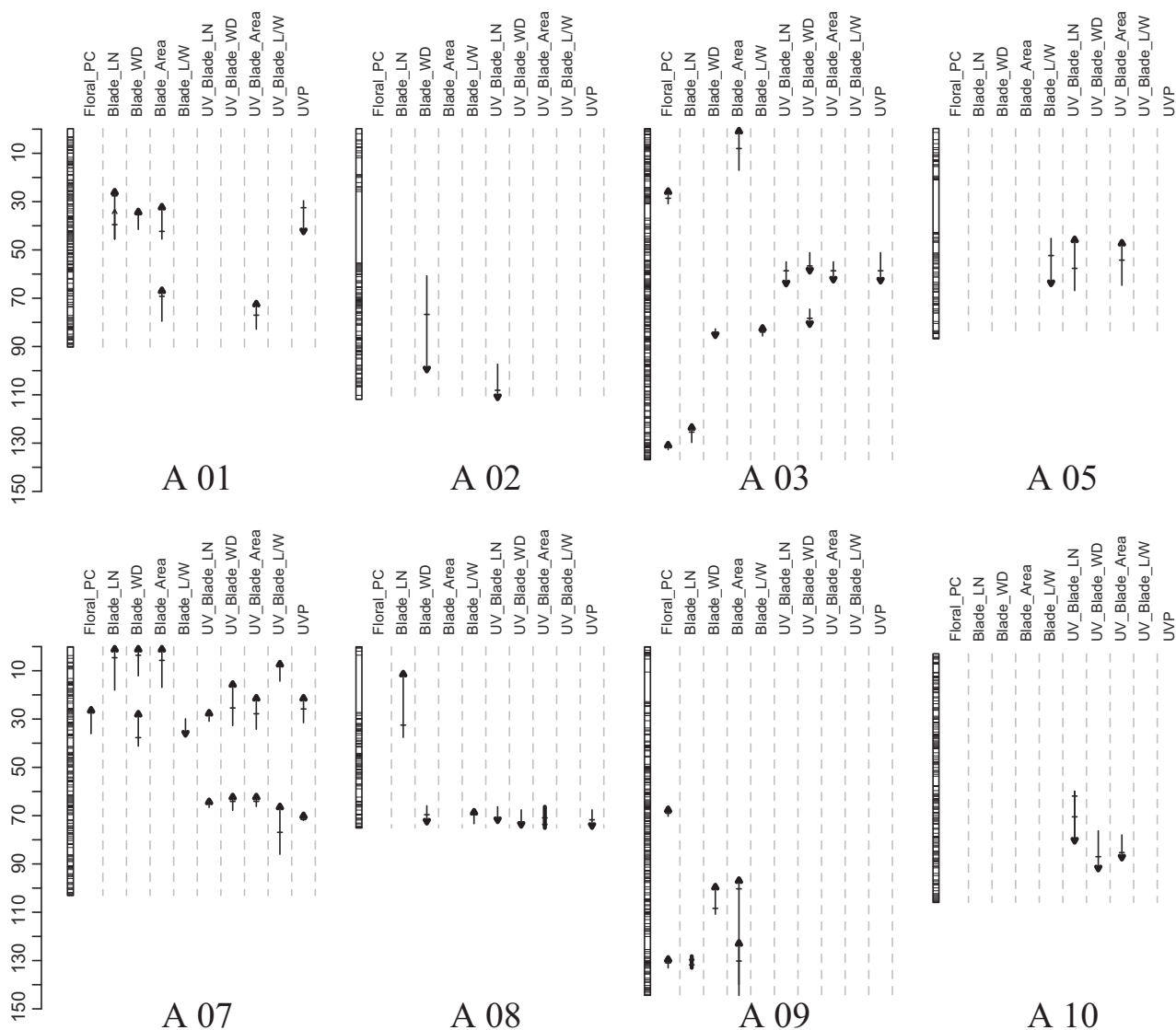


Fig. 2 Genomic locations of QTL regulating size and shape of floral whorl, petal blade and petal UV region traits of *B. rapa* RILs. QTL peaks are illustrated with short horizontal lines perpendicular to the vertical 2-LOD support limits. Arrowheads indicate the positive (up) or negative (down) additive effect on trait means from the inheritance of an R500 allele.

isorhamnetin flavonoid described by Sasaki & Takahashi (2002) as underlying the UV patterning in *B. rapa*. LC-MS confirms that peak 4 is isorhamnetin (mass 641.1719; chemical formula $C_{28}H_{33}O_{17}$).

In comparison with R500, IMB211 has on average 73.9% higher concentration of sinapoyl glucose (genotype; $F_{1,12} = 5.18$, P -value = 0.0419); moreover, both genotypes have on average 5.2 times more sinapoyl glucose in the UV-absorbing regions of the petal blade in comparison with the reflecting apical petal tips (petal region; $F_{1,12} = 32.43$, P -value < 0.0001; Fig. 3A). Genotypes did not differ significantly in their patterning of sinapoyl glucose concentration across UV-absorbing and UV-reflecting petal regions

(genotype \times petal region interaction; $F_{1,12} = 0.38$, P -value = 0.55). We detect a significant genotype \times petal region interaction for the concentration of isorhamnetin (genotype \times petal region interaction; $F_{1,12} = 9.43$, P -value = 0.0097). Post hoc tests indicate that while isorhamnetin concentrations in IMB211 trend in the direction of the UV pattern (i.e. higher concentrations in UV-absorbing petal regions), they are only marginally different (Tukey's test, P -value = 0.072; Fig. 3B). Isorhamnetin concentrations in the UV-reflecting regions in R500 are greater than those in the UV-absorbing regions (i.e. counter to the observed UV pattern); however, they are not significantly different (Tukey's test, P -value = 0.42; Fig. 3B).

Influence of UV patterns on insect visitation

Insect visitation at the whole plant and flower level was influenced significantly by UV experimental treatments (Table 4, Fig. 4). Insect visitation at both the plant and flower level did not differ between control and duck fat treatments (i.e. both treatments had UV-patterned flowers; Tukey's test, P -value = 0.99 and 0.48, respectively). Alternatively, plants with UV-patterned flowers received 1.6× more insect visits than those with completely UV-absorbing flowers (Tukey's tests, P -value <0.008) and total visits to UV-patterned flowers were two times greater than those that lacked a UV pattern (Tukey's test, P -value <0.02).

Discussion

Nectar guides are commonly found on angiosperm flowers and have been shown to enhance the frequency and efficiency of insect visitation as well as the efficiency of pollen transfer and seed set (Waser & Price 1985; Leonard & Papaj 2011; Hansen *et al.* 2012). We find variation in the expression of a UV bulls-eye pattern within and among wild and crop genotypes of *B. rapa*. We also detect significant genetic variation in the size and shape of UV patterns in a segregating progeny established by crossing parents with UV bulls-eye

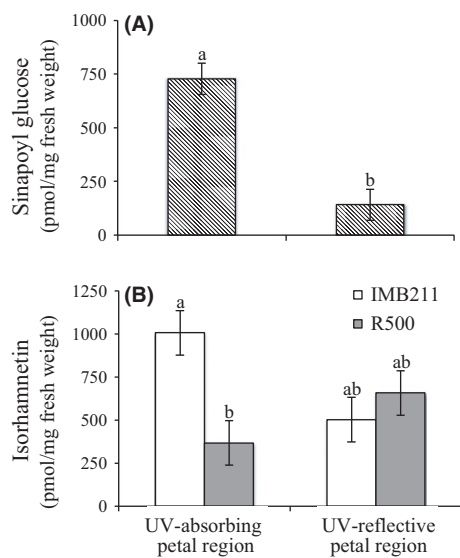


Fig. 3 Concentrations of (A) sinapoyl glucose and (B) isorhamnetin in UV-absorbing or UV-reflecting petal blade regions of *Brassica rapa*. Sinapoyl glucose concentrations were averaged over the two parental genotypes, R500 and IMB211, in panel A, because the genotype × tissue region interaction was non-significant. Isorhamnetin concentrations shown in panel B illustrate the significant genotype × tissue region interaction. Letters denote significant differences at P -value <0.0001 and P -value <0.02 for panels A and B, respectively.

Table 4 Mixed-model ANCOVA results partitioning variance in two measures of visitation among pollinators (megachilids and all other hymenopterans), UV treatments (control, UV+ and UV-) and the pollinator by UV treatment interaction, while controlling for spatial blocks, temporal blocks and the total number of flowers per experimental plant

Fixed effects	Total visits to plants		Total visits to flowers	
	d.f.	F-value	d.f.	F-value
Total floral display	1, 119	0.07	1, 90	4.35*
Pollinators	1, 139	0.08	1, 147	0.05
UV treatments	2, 124	5.92**	2, 129	8.06***
Pollinator × UV Trt	2, 126	0.92	2, 131	1.45
Random effects	Z-value		Z-value	
Block (Date)		2.5**		0.96
Date		NE		NE

NE, not estimable.

*<0.05; **<0.01; ***<0.001.

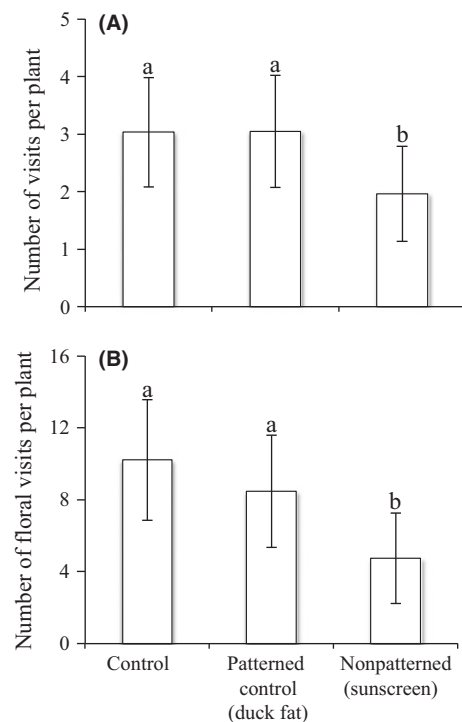


Fig. 4 Least-squared means of the number of insect visits to (A) plants or (B) flowers, of those plants, in UV experimental treatments. Treatments consisted of control (unmanipulated), patterned controls (duck fat on petal blades) and nonpatterned flowers (sunscreen in duck fat applied to petal blades). Letters denote significant differences among treatments with P -value <0.008 and P -value <0.015 for panels A and B, respectively.

patterns. While there are strong genetic correlations within petal size traits (length, width and area) or within size measures of the UV bulls-eye region, correlations across these two groups of petal traits are considerably weaker or not significant; QTL results likewise suggest genetic independence of these groups of petal traits. Analyses of secondary compounds show that sinapoyl glucose, a UV-absorbing phenylpropanoid compound, has consistently higher concentrations in UV-absorbing petal blade regions of both parents of the RIL population. Considering the biochemical pathway and relating our genetic map to the physical map, bioinformatic analyses suggest variation at both regulatory and structural genes may contribute to interindividual variation, although this awaits functional confirmation. Finally, using one of the RIL parents, we find that insect visitation increases twofold for plants with UV patterns in comparison with those with experimentally engineered patternless flowers; this result validates the importance of nectar guides to plant–pollinator interactions in this system and the ecological relevance of characterizing the genetic architecture and causal loci, but raises the question of why UV patterning is lacking in most wild populations.

Phenotypic and genetic variation in floral UV patterning

Previous studies have only reported that flowers of *B. rapa* (Sasaki & Takahashi 2002; Yoshioka *et al.* 2005) and of close *Brassica* relatives (*B. nigra* and *B. oleracea*; Horovitz & Cohen 1972) have UV bulls-eye patterns. In our limited genotypic survey, wild populations and crop accessions vary in the presence vs. absence of UV bulls-eye patterns. Vegetable (leaf and root) crops of *B. rapa* exhibit UV patterning as do most (72% of) floral and oilseed genotypes. Volunteer wild populations of *B. rapa* in western North America predominantly lack UV bulls-eye patterns, having flowers that are uniformly absorbing in the near-UV spectrum. This qualitative variation in UV patterning is interesting given the number of studies (including this one) that suggest benefits of nectar guides to plant–pollinator interactions. Founder effects, from one to few crop populations, could explain the overrepresentation of this phenotype in a non-native range (e.g. Eckert *et al.* 1996). In this regard, it is worth noting that the North American wild populations may derive from oilseed or broccoletto crops, because the wild populations resemble these crops in both morphology (which is distinct from the high root and leaf allocation of vegetable crops) and life history (as the wild populations lack a vernalization requirement common to vegetable crops); oilseeds and broccolettos also occasionally lack UV patterns. The

rarity of UV patterns in North American populations could, alternatively, be adaptive if this phenotype reduces floral apparency to herbivorous insects (Cook *et al.* 2013; Perez-Barrales *et al.* 2013) or if UV-absorbing floral pigments (e.g. dearomatized isoprenylated phloroglucinols) deter florivores (Gronquist *et al.* 2001). Finally, the absence of UV patterns might be attributable to selection on flavonoids in other plant organs (e.g. selection for cold tolerance in leaves) that leads to a correlated response in flowers (Dick *et al.* 2011; Ahmed *et al.* 2014). A larger genotypic survey (and more extensive sampling within populations) would help discriminate between geographic vs. domestication effects on floral UV patterning and could provide insights as to selective agents other than pollinators acting on UV-absorbing compounds.

In addition to qualitative variation in UV patterning, segregating progeny between two UV bulls-eye-patterned parents exhibit extensive genetic variation for the size and shape of petal UV regions. Our results support the highly heritable nature of UV nectar guide size, shape and UVP (average $H^2 = 0.45$; Table 2), and while the broad-sense heritability estimates of UV size and UVP traits were lower than those reported in recent greenhouse studies (e.g. $H^2 = \sim 0.75$ and ~ 0.85 ; Koski & Ashman 2013; respectively; Syafaruddin *et al.* 2006), plants in our experiment were raised under more variable and realistic field conditions that induce higher levels of UV-absorbing compounds. We also detect significant genetic variation for petal blade morphology and allometry, supporting previous examinations of floral genetic architecture in this population (Brock *et al.* 2010). More interestingly, while there are strong positive genetic correlations within size traits of petal blades OR of petal UV regions, the correlation structure across these two suites of traits is considerably weaker or not significant (Table 3, Fig. S2, Supporting information). Similarly, we find weak correlation structure between UV traits and the size of other floral whorls (i.e. floral size PC). Taken together, UV region size traits are genetically decoupled from floral size traits. A similarly weak correlation structure was observed in *Argentina anserina* (Rosaceae; Koski & Ashman 2013), suggesting that development of petals and their nectar guide patterns are likely to be regulated by independent genetic mechanisms in many angiosperms.

Our genomewide scans revealed numerous QTL regulating floral size, shape and UV patterning traits and support a disassociated petal blade and UV-pattern genetic architecture. We detected up to 10 main-effect and two-way epistatic QTL regulating UV-pattern traits, many of which regulate only UV-pattern features and not petal blade traits. These QTL explain $\sim 50\%$ of segregating genetic variation after tallying individual (and

interactive) effect sizes, which suggests additional main-effect and multiway epistatic interactions of small effect size likely account for the residual genetic variance. Petal blade traits are regulated by at least five QTL of overlapping effect (e.g. bottom of A09, Fig. 2), which likely arise from pleiotropic genes that influence multiple traits (although we cannot discount linkage disequilibrium between physically proximate genes). While UV-pattern traits are often regulated by distinct pleiotropic QTL (e.g. bottom of A07, Fig. 2), we do detect a QTL that affects both petal morphology and UV patterning (e.g. the 'hotspot' at the bottom of A08; Fig. 2). Overall, the QTL architecture supports the strong positive genetic correlations observed *within* petal blade morphology and UV region traits, while accounting for the weaker correlations observed *between* petal blade and UV-pattern size traits. This dissociated genetic architecture is most evident for UV shape (UV L/W) and UVP traits, for which there is only evidence for a weak correlation between UVP and either petal blade size or shape (L/W). Thus, if UV shape or UVP traits are favoured in pollen-limited natural populations with floral genetic architectures similar to that of the experimental population used here, they should evolve independently of selection acting on floral size traits (e.g. pollinator attraction via petal blade size).

Phenylpropanoid compounds underlying nectar guide patterning

Previous examination of UV nectar guides in other genera (e.g. *Rudbeckia*, *Hypericum* and *Oenothera*; Dement & Raven 1974; Gronquist *et al.* 2001; Thompson *et al.* 1972) has found that UV-absorbing flavonoids determine UV nectar guide patterning and accordingly are in higher concentration in the bulls-eye region of patterned flowers. Of the several compounds that exhibit differential absorbance profiles across UV-absorbing and UV-reflecting petal blade regions in the current study, only concentrations of sinapoyl glucose, a phenolic that absorbs wavelengths in the UV spectrum to which insects are commonly sensitive (i.e. 330–360 nm; Briscoe & Chittka 2001), correlate consistently with visualized UV patterns in both genotypes analysed. Isorhamnetin, a flavonoid compound that was previously identified as responsible for the UV nectar guide in *B. rapa* (Sasaki & Takahashi 2002), is more variable in its concentration across petal regions in our *Brassica* plants; while it trends in the same direction as the UV patterning in one *Brassica* genotype (IMB211; Fig 4B), we find that isorhamnetin concentrations do not differ between reflective and absorbing regions of R500. Environmental upregulation of phenylpropanoid compounds might contribute to experimental differences;

Sasaki & Takahashi (2002) raised plants in the greenhouse for the most part, while plants in the current study were raised in the field. Genetic variation across subspecies could also be important; Sasaki & Takahashi (2002) examined UV patterning in flowers of Chinese cabbage (subsp., *pekinensis*) while we examined oilseeds (subsp., *oleifera*). Causal compounds may also be genotype specific; while isorhamnetin does not contribute to patterning in R500, it may do so in IMB211 or other genotypes of *B. rapa*.

The phenylpropanoid biochemical pathways that produce human-visible and UV-spectral pigments (e.g. anthocyanins, flavonoids, sinapate esters) are well characterized; however, the molecular genetic dissection of pigment patterning has, for obvious reasons, been examined predominantly for human-visible pigments and only in recent years. Examination of mutant phenotypes in the model organisms *Antirrhinum*, *Petunia* and *Mimulus* (Schwinn *et al.* 2006; Albert *et al.* 2011; Shang *et al.* 2011; Yuan *et al.* 2013b) has consistently revealed R2R3-MYB factors as key regulators of both variation in overall floral colour (e.g. pink vs. blue) and floral pigment patterning (e.g. anthocyanic lines and spots). MYB factors form a regulatory complex with two additional proteins, WD40 and bHLH repeat proteins, and although there are examples of bHLH mutants influencing pigment patterning (e.g. the *Antirrhinum* bHLH Delila mutant; Goodrich *et al.* 1992), the greater pleiotropic effects of these latter two elements suggest that the subtle control of anthocyanic pigment patterning may arise more often from MYB factors (Streisfeld *et al.* 2011; Yuan *et al.* 2014).

Although sinapate esters branch from the pathway that produces anthocyanins, MYB factors, along with UGTs (UDP-glucosyltransferases), have also been shown to regulate sinapate glucose production (Jin *et al.* 2000; Hemm *et al.* 2001). Examination of genes within support limits surrounding three highly resolved QTL that regulate the size of UV traits and UVP (see middle of A03 and bottom of A07 and A08; Fig. 2) reveals several genes in MYB, WD, bHLH and UGT candidate families; however, sequence and functional characterization places most of these candidates in gene family subgroups other than those regulating phenylpropanoid metabolism. We did identify two strong candidates that are homologous to *Arabidopsis thaliana* phenylpropanoid genes. Under the QTL3-3 peak on A03, we detected a gene homologous to MYB12 in *Arabidopsis thaliana* (PFG1; At2g47460), which targets genes that lead to flavonoid biosynthesis (e.g. 4CL3 and chalcone synthase; Stracke *et al.* 2007) as well as a UDP-glucosyltransferase gene similar to UGT84A1 from *A. thaliana*. Along with other closely related UGT genes, UGT84A1 forms glucose esters of sinapic acid and is expressed predomi-

nantly in roots, shoot apex, flowers and seeds (Lim *et al.* 2001; Meßner *et al.* 2003; Schmid *et al.* 2005). The second candidate is the structural gene, *4CL3*, underlying QTL7-3; this ligase catalyses the conversion of *p*-coumaric acid to *p*-coumaroyl CoA, an early precursor in the production of many phenylpropanoid compounds, including sinapoyl glucose (Milkowski & Strack 2010). In addition to *UGT84A1*, *MYB12* has been shown to target *4CL3* (Stracke *et al.* 2001) and all three genes are highly co-expressed in *Arabidopsis* expression databases (Obayashi *et al.* 2011). Moreover, R500 and IMB211 have nonsynonymous substitutions in alleles of both candidate genes; this amino acid variation is proximal to putative functional domains in the *Brassica* homologs of *MYB12* and *4CL3*, respectively (Schneider *et al.* 2003; Stracke *et al.* 2007; Czemplak *et al.* 2009; Sigris *et al.* 2013), and may influence quantitative variation in UV-pattern traits via shifts in protein function.

Given these functional characterizations and gene expression data in *A. thaliana*, the *B. rapa* homologs of *MYB12* and *4CL3* are logical candidates for future fine-scale mapping or expression studies exploring UV patterning in *B. rapa*. More generally, the increase in marker density in this map (via short-read sequencing of expressed genes) relative to earlier linkage maps in combination with functional and bioinformatic screens illustrates how candidate gene identification may be improved. Development of a novel RIL population from parents that either entirely lack (wild parent, Fig. 1D) or show (oilseed parent, Fig. 1E) floral UV patterning is in progress and will also improve the genetic dissection of this trait.

Plant–pollinator interactions and floral evolution

Nectar guides influence the behaviour of floral visitors. Studies of both artificial models and experimentally manipulated flowers have shown that insects commonly prefer patterned flowers (Hansen *et al.* 2012; Koski & Ashman 2014; Peterson *et al.* 2015) and that nectar guides can enhance the efficiency and frequency of insect visits (Waser & Price 1985; Leonard *et al.* 2013). Our experimental manipulations of *B. rapa* flowers support these previous studies; Megachilids, and hymenopterans in general, visit flowers with UV nectar guides twice as often as those without them (Fig. 4). All hymenopterans, except for ants, are known to have some level of UV sensitivity, and many members of the Megachilidae (e.g. *Osmia rufa* and *Anthidium manicatum*) are predicted to have maximum UV sensitivity near 355 nm (Briscoe & Chittka 2001). These behavioural responses could be innate as has been demonstrated for naïve honeybees and bumblebees visiting model flowers (Free 1970; Leonard & Papaj 2011) or alternatively may

be learned behaviours in response to variation in UV patterning of the local flowering community at the time of our experiment. In addition to the yellow colour of *Brassica rapa* petals (bee-green and bee-UV-green; Chittka 1992), which has been shown to be favoured by bumblebees due to higher contrast with foliar backgrounds (Spaethe *et al.* 2001; Simonds & Plowright 2004), the UV wavelengths reflected by the petal apex (bee-UV-green) should provide visual contrast relative to the UV-absorbing background vegetation (bee-uncoloured). This UV contrast at petal apices may facilitate floral apparency to approaching insect visitors, while the internal contrast between UV-reflecting and UV-absorbing petal regions may facilitate insects moving from floral edges to the central rewards (Lunau *et al.* 2006).

Our phenotypic engineering of UV patterning tested for insect preferences to discrete UV phenotypes and results suggest that, in pollen-limited populations, selection mediated through insect preference favours UV patterning (this study) likely in combination with larger petals or floral display (Mitchell *et al.* 2004; Harder & Johnson 2009; Parachnowitsch & Kessler 2010). In addition to insect preference for qualitative variation in UV patterning, it would be interesting to explore how the more subtle quantitative variation in UVP observed in our segregating progeny influences insect visitation (Koski & Ashman 2015). Correlations between the UVP and floral/petal size traits are nonsignificant here, indicating these traits could evolve to the optimum. However, selection can act on floral shape or symmetry (Galen & Cuba 2001; Gomez *et al.* 2006), and the negative correlation observed between petal shape (blade L/W) and UVP could affect the joint evolution of these two attraction traits.

In the light of insect preference for UV-patterned *B. rapa* flowers, it is again surprising that North American wild populations predominantly lack UV patterns. While founder effects in these introduced populations may account for the rarity of UV patterns, selection may also play a role if increased floral expression of sinapate esters (or flavonoids) enhances protection for male or female gametes (Koski & Ashman 2015) or if these UV-absorbing compounds deter florivores or seed predators (Perez-Barrales *et al.* 2013). Our current crosses in development between UV-patterned and patternless genotypes should illuminate the chemical nature, inheritance and underlying genetic architecture of these discrete phenotypes and facilitate the examination of the selective benefits of variation in UV nectar guides.

Acknowledgments

The authors appreciate the help of numerous undergraduate and graduate students at the University of Wyoming including

S. Anderson, D. Lorimer, D. Nykodym, M. Pratt, K. Riggs, L. Steinken, A. Wagner, S. Wakefield, B. Wehmeyer and R. Winkelman; the assistance of R. Hartman and B. E. Nelson of the Rocky Mountain Herbarium; and the maintenance of greenhouse and field plants by R. Pendleton, C. Seals and E. Walter. This research was supported by NSF grant IOS-0923752 to CW and JNM.

References

- Ahmed NU, Park JI, Jung HJ *et al.* (2014) Characterization of dihydroflavonol 4-reductase (*DFR*) genes and their association with cold and freezing stress in *Brassica rapa*. *Gene*, **550**, 46–55.
- Albert NW, Lewis DH, Zhang H *et al.* (2011) Members of an R2R3-MYB transcription factor family in *Petunia* are developmentally and environmentally regulated to control complex floral and vegetative pigmentation patterning. *Plant Journal*, **65**, 771–784.
- Altschul SF, Madden TL, Schaffer AA *et al.* (1997) Gapped BLAST and PSI-BLAST: a new generation of protein database search programs. *Nucleic Acids Research*, **25**, 3389–3402.
- Bateman AJ (1955) Self-incompatibility systems in angiosperms. III. Cruciferae. *Heredity*, **9**, 52–68.
- Box GEP, Cox DR (1964) An analysis of transformations. *Journal of the Royal Statistical Society Series B-Statistical Methodology*, **26**, 211–252.
- Bradshaw HD, Schemske DW (2003) Allele substitution at a flower colour locus produces a pollinator shift in monkeyflowers. *Nature*, **426**, 176–178.
- Briscoe AD, Chittka L (2001) The evolution of color vision in insects. *Annual Review of Entomology*, **46**, 471–510.
- Brock MT, Dechaine JM, Iniguez-Luy FL *et al.* (2010) Floral genetic architecture: an examination of QTL architecture underlying floral (co)variation across environments. *Genetics*, **186**, 1451–1465.
- Broman KW, Wu H, Sen ÁACG (2003) R/qtl: QTL mapping in experimental crosses. *Bioinformatics*, **19**, 889–890.
- Buer CS, Imin N, Djordjevic MA (2010) Flavonoids: new roles for old molecules. *Journal of Integrative Plant Biology*, **52**, 98–111.
- Carey CC, Strahle JT, Selinger DA, Chandler VL (2004) Mutations in the *pale aleurone color1* regulatory gene of the *Zea mays* anthocyanin pathway have distinct phenotypes relative to the functionally similar *TRANSPARENT TESTA GLABRA1* gene in *Arabidopsis thaliana*. *Plant Cell*, **16**, 450–464.
- Chapple CCS, Vogt T, Ellis BE, Somerville CR (1992) An *Arabidopsis* mutant defective in the general phenylpropanoid pathway. *Plant Cell*, **4**, 1413–1424.
- Chittka L (1992) The color hexagon: a chromaticity diagram based on photoreceptor excitations as a generalized representation of color opponency. *Journal of Comparative Physiology A*, **170**, 533–543.
- Churchill GA, Doerge RW (1994) Empirical threshold values for quantitative trait mapping. *Genetics*, **138**, 963–971.
- Cook SM, Skellern MP, Doring TF, Pickett JA (2013) Red oil-seed rape? The potential for manipulation of petal colour in control strategies for the pollen beetle (*Meligethes aeneus*). *Arthropod-Plant Interactions*, **7**, 249–258.
- Czemmel S, Stracke R, Weisshaar B *et al.* (2009) The grapevine R2R3-MYB transcription factor VvMYBF1 regulates flavonol synthesis in developing grape berries. *Plant Physiology*, **151**, 1513–1530.
- Dafni A, Kevan PG (1996) Floral symmetry and nectar guides: ontogenetic constraints from floral development, colour pattern rules and functional significance. *Botanical Journal of the Linnean Society*, **120**, 371–377.
- Dement WA, Raven PH (1974) Pigments responsible for ultraviolet patterns in flowers of *Oenothera* (Onagraceae). *Nature*, **252**, 705–706.
- Devisetty UK, Covington MF, Tat AV, Lekkala S, Maloof JN (2014) Polymorphism identification and improved genome annotation of *Brassica rapa* through deep RNA sequencing. *G3: Genes|Genomes|Genetics*, **4**, 2065–2078.
- Dick CA, Buenrostro J, Butler T *et al.* (2011) Arctic mustard flower color polymorphism controlled by petal-specific downregulation at the threshold of the anthocyanin biosynthetic pathway. *PLoS ONE*, **6**, e18230.
- Domb LG, Pagel M (2001) Sexual swellings advertise female quality in wild baboons. *Nature*, **410**, 204–206.
- Dubos C, Stracke R, Grotewold E *et al.* (2010) MYB transcription factors in *Arabidopsis*. *Trends in Plant Science*, **15**, 573–581.
- Dyer AG (1996) Reflection of near-ultraviolet radiation from flowers of Australian native plants. *Australian Journal of Botany*, **44**, 473–488.
- Eckert CG, Manicacci D, Barrett SCH (1996) Genetic drift and founder effect in native versus introduced populations of an invading plant, *Lythrum salicaria* (Lythraceae). *Evolution*, **50**, 1512–1519.
- Etterson JR, Shaw RG (2001) Constraint to adaptive evolution in response to global warming. *Science*, **294**, 151–154.
- Falconer DS, Mackay TFC (1996) *Introduction to Quantitative Genetics*. Longman, Harlow, U.K.
- Fraser CM, Thompson MG, Shirley AM *et al.* (2007) Related *Arabidopsis* serine carboxypeptidase-like sinapoylglucose acyltransferases display distinct but overlapping substrate specificities. *Plant Physiology*, **144**, 1986–1999.
- Free JB (1970) Effect of flower shapes and nectar guides on the behaviour of foraging honeybees. *Behaviour*, **37**, 269–285.
- Galen C (1996) Rates of floral evolution: adaptation to bumblebee pollination in an alpine wildflower. *Polemonium viscosum*, **50**, 120–125.
- Galen C, Cuba J (2001) Down the tube: pollinators, predators, and the evolution of flower shape in the alpine skypilot, *Polemonium viscosum*. *Evolution*, **55**, 1963–1971.
- Glaetli M, Barrett SCH (2008) Pollinator responses to variation in floral display and flower size in dioecious *Sagittaria latifolia* (Alismataceae). *New Phytologist*, **179**, 1193–1201.
- Gomez JM, Perfectti F, Camacho JPM (2006) Natural selection on *Erysimum mediohispanicum* flower shape: insights into the evolution of zygomorphy. *American Naturalist*, **168**, 531–545.
- Goodrich J, Carpenter R, Coen ES (1992) A common gene regulates pigmentation pattern in diverse plant species. *Cell*, **68**, 955–964.
- Gronquist M, Bezzerides A, Attygalle A *et al.* (2001) Attractive and defensive functions of the ultraviolet pigments of a flower (*Hypericum calycinum*). *Proceedings of the National Academy of Sciences of the United States of America*, **98**, 13745–13750.
- Hansen DM, Van der Niet T, Johnson SD (2012) Floral signposts: testing the significance of visual ‘nectar guides’ for

- pollinator behaviour and plant fitness. *Proceedings of the Royal Society B-Biological Sciences*, **279**, 634–639.
- Harder LD, Johnson SD (2009) Darwin's beautiful contrivances: evolutionary and functional evidence for floral adaptation. *New Phytologist*, **183**, 530–545.
- Heim MA, Jakoby M, Werber M *et al.* (2003) The basic helix-loop-helix transcription factor family in plants: a genome-wide study of protein structure and functional diversity. *Molecular Biology and Evolution*, **20**, 735–747.
- Hemm MR, Herrmann KM, Chapple C (2001) AtMYB4: a transcription factor general in the battle against UV. *Trends in Plant Science*, **6**, 135–136.
- Henikoff S, Henikoff JG (1992) Amino acid substitution matrices from protein blocks. *Proceedings of the National Academy of Sciences of the United States of America*, **89**, 10915–10919.
- Hoballah ME, Gubitza T, Stuurman J *et al.* (2007) Single gene-mediated shift in pollinator attraction in *Petunia*. *Plant Cell*, **19**, 779–790.
- Holm L, Doll J, Holm E, Pancho J, Herberger J (1997) *World Weeds: Natural Histories and Distribution*. John Wiley & Sons Inc, New York, New York, USA.
- Holton TA, Cornish EC (1995) Genetics and biochemistry of anthocyanin biosynthesis. *Plant Cell*, **7**, 1071–1083.
- Horovitz A, Cohen Y (1972) Ultraviolet reflectance characteristics in flowers of crucifers. *American Journal of Botany*, **59**, 706–713.
- Iniguez-Luy FL, Lukens L, Farnham MW, Amasino RM, Osborn TC (2009) Development of public immortal mapping populations, molecular markers and linkage maps for rapid cycling *Brassica rapa* and *B. oleracea*. *Theoretical and Applied Genetics*, **120**, 31–43.
- Jin HL, Cominelli E, Bailey P *et al.* (2000) Transcriptional repression by AtMYB4 controls production of UV-protecting sunscreens in *Arabidopsis*. *Embo Journal*, **19**, 6150–6161.
- Johnson SD, Andersson S (2002) A simple field method for manipulating ultraviolet reflectance of flowers. *Canadian Journal of Botany-Revue Canadienne De Botanique*, **80**, 1325–1328.
- Johnson SD, Midgley JJ (1997) Fly pollination of *Gorteria diffusa* (Asteraceae), and a possible mimetic function for dark spots on the capitulum. *American Journal of Botany*, **84**, 429–436.
- Jones IL, Hunter FM (1993) Mutual sexual selection in a monogamous seabird. *Nature*, **362**, 238–239.
- Kevan PG, Chittka L, Dyer AG (2001) Limits to the salience of ultraviolet: lessons from colour vision in bees and birds. *Journal of Experimental Biology*, **204**, 2571–2580.
- Koski MH, Ashman TL (2013) Quantitative variation, heritability, and trait correlations for ultraviolet floral traits in *Argentina anserina* (Rosaceae): implications for floral evolution. *International Journal of Plant Sciences*, **174**, 1109–1120.
- Koski MH, Ashman TL (2014) Dissecting pollinator responses to a ubiquitous ultraviolet floral pattern in the wild. *Functional Ecology*, **28**, 868–877.
- Koski MH, Ashman T-L (2015) Floral pigmentation patterns provide an example of Gloger's rule in plants. *Nature Plants*, **1**, 14007.
- Lee S, Kaminaga Y, Cooper B *et al.* (2012) Benzoylation and sinapoylation of glucosinolate R-groups in *Arabidopsis*. *Plant Journal*, **72**, 411–422.
- Leonard AS, Papaj DR (2011) 'X' marks the spot: the possible benefits of nectar guides to bees and plants. *Functional Ecology*, **25**, 1293–1301.
- Leonard AS, Brent J, Papaj DR, Dornhaus A (2013) Floral nectar guide patterns discourage nectar robbing by bumble bees. *PLoS ONE*, **8**, e55914.
- Li Y, Baldauf S, Lim EK, Bowles DJ (2001) Phylogenetic analysis of the UDP-glycosyltransferase multigene family of *Arabidopsis thaliana*. *Journal of Biological Chemistry*, **276**, 4338–4343.
- Li X, Bergelson J, Chapple C (2010) The *ARABIDOPSIS* accession Pna-10 is a naturally occurring *sng1* deletion mutant. *Molecular Plant*, **3**, 91–100.
- Lim EK, Li Y, Parr A *et al.* (2001) Identification of glucosyltransferase genes involved in sinapate metabolism and lignin synthesis in *Arabidopsis*. *Journal of Biological Chemistry*, **276**, 4344–4349.
- Lunau K (1990) Color saturation triggers innate reactions to flower signals: flower dummy experiments with bumblebees. *Journal of Comparative Physiology A*, **166**, 827–834.
- Lunau K, Fieselmann G, Heuschen B, van de Loo A (2006) Visual targeting of components of floral colour patterns in flower-naïve bumblebees (*Bombus terrestris*; Apidae). *Naturwissenschaften*, **93**, 325–328.
- Matsubara K, Kei S, Koizumi M, Kodama H, Ando T (2012) RNA silencing in white petunia flowers creates pigmentation patterns invisible to the human eye. *Journal of Plant Physiology*, **169**, 920–923.
- Medel R, Botto-Mahan C, Kalin-Arroyo M (2003) Pollinator-mediated selection on the nectar guide phenotype in the Andean monkey flower, *Mimulus luteus*. *Ecology*, **84**, 1721–1732.
- Meßner B, Thulke O, Schäffner AR (2003) Arabidopsis glucosyltransferases with activities toward both endogenous and xenobiotic substrates. *Planta*, **217**, 138–146.
- Milkowski C, Strack D (2010) Sinapate esters in brassicaceous plants: biochemistry, molecular biology, evolution and metabolic engineering. *Planta*, **232**, 19–35.
- Mitchell RJ, Karron JD, Holmquist KG, Bell JM (2004) The influence of *Mimulus ringens* floral display size on pollinator visitation patterns. *Functional Ecology*, **18**, 116–124.
- Møller AP (1995) Bumblebee preference for symmetrical flowers. *Proceedings of the National Academy of Sciences of the United States of America*, **92**, 2288–2292.
- Nou IS, Watanabe M, Isuzugawa K, Isogai A, Hinata K (1993) Isolation of S-alleles from a wild population of *Brassica campestris* L. at Balcesme, Turkey and their characterization by S-glycoproteins. *Sexual Plant Reproduction*, **6**, 71–78.
- Obayashi T, Nishida K, Kasahara K, Kinoshita K (2011) ATTED-II updates: condition-specific gene coexpression to extend coexpression analyses and applications to a broad range of flowering plants. *Plant and Cell Physiology*, **52**, 213–219.
- Pang YZ, Wenger JP, Saathoff K *et al.* (2009) A WD40 repeat protein from *Medicago truncatula* is necessary for tissue-specific anthocyanin and proanthocyanidin biosynthesis but not for trichome development. *Plant Physiology*, **151**, 1114–1129.
- Parachnowitsch AL, Kessler A (2010) Pollinators exert natural selection on flower size and floral display in *Penstemon digitalis*. *New Phytologist*, **188**, 393–402.
- Pattanaik S, Kong Q, Zaitlin D *et al.* (2010) Isolation and functional characterization of a floral tissue-specific R2R3 MYB regulator from tobacco. *Planta*, **231**, 1061–1076.

- Penny JHJ (1983) Nectar guide color contrast: a possible relationship with pollination strategy. *New Phytologist*, **95**, 707–721.
- Perez-Barrales R, Bolstad GH, Pelabon C, Hansen TF, Armbruster WS (2013) Pollinators and seed predators generate conflicting selection on *Dalechampia* blossoms. *Oikos*, **122**, 1411–1428.
- Peterson ML, Miller TJ, Kay KM (2015) An ultraviolet floral polymorphism associated with life history drives pollinator discrimination in *Mimulus guttatus*. *American Journal of Botany*, **102**, 396–406.
- Ramsay NA, Glover BJ (2005) MYB-bHLH-WD40 protein complex and the evolution of cellular diversity. *Trends in Plant Science*, **10**, 63–70.
- Sasaki K, Takahashi T (2002) A flavonoid from *Brassica rapa* flower as the UV-absorbing nectar guide. *Phytochemistry*, **61**, 339–343.
- Schluter D (1996) Adaptive radiation along genetic lines of least resistance. *Evolution*, **50**, 1766–1774.
- Schmid M, Davison TS, Henz SR *et al.* (2005) A gene expression map of *Arabidopsis thaliana* development. *Nature Genetics*, **37**, 501–506.
- Schneider K, Hovel K, Witzel K *et al.* (2003) The substrate specificity-determining amino acid code of 4-coumarate: CoA ligase. *Proceedings of the National Academy of Sciences of the United States of America*, **100**, 8601–8606.
- Schwinn K, Venail J, Shang YJ *et al.* (2006) A small family of MYB-regulatory genes controls floral pigmentation intensity and patterning in the genus *Antirrhinum*. *Plant Cell*, **18**, 831–851.
- Shang YJ, Venail J, Mackay S *et al.* (2011) The molecular basis for venation patterning of pigmentation and its effect on pollinator attraction in flowers of *Antirrhinum*. *New Phytologist*, **189**, 602–615.
- Sigrist CJA, de Castro E, Cerutti L *et al.* (2013) New and continuing developments at PROSITE. *Nucleic Acids Research*, **41**, E344–E347.
- Simonds V, Plowright CMS (2004) How do bumblebees first find flowers? unlearned approach responses and habituation. *Animal Behaviour*, **67**, 379–386.
- Sobel JM, Streisfeld MA (2013) Flower color as a model system for studies of plant evo-devo. *Frontiers in plant science*, **4**, 321.
- Sokal RR, Rohlf FJ (1995) *Biometry. The Principles and Practice of Statistics in Biological Research*, 3rd edn. W. H. Freeman, New York, New York, USA.
- Spaethe J, Tautz J, Chittka L (2001) Visual constraints in foraging bumblebees: flower size and color affect search time and flight behavior. *Proceedings of the National Academy of Sciences of the United States of America*, **98**, 3898–3903.
- Stracke R, Werber M, Weisshaar B (2001) The R2R3-MYB gene family in *Arabidopsis thaliana*. *Current Opinion in Plant Biology*, **4**, 447–456.
- Stracke R, Ishihara H, Barsch GHA *et al.* (2007) Differential regulation of closely related R2R3-MYB transcription factors controls flavonol accumulation in different parts of the *Arabidopsis thaliana* seedling. *Plant Journal*, **50**, 660–677.
- Streisfeld MA, Liu D, Rausher MD (2011) Predictable patterns of constraint among anthocyanin-regulating transcription factors in *Ipomoea*. *New Phytologist*, **191**, 264–274.
- Syafaruddin, Kobayashi K, Yoshioka Y *et al.* (2006) Estimation of heritability of the nectar guide of flowers in *Brassica rapa* L. *Breeding Science*, **56**, 75–79.
- Thompson WR, Aneshans D, Meinwald J, Eisner T (1972) Flavonols: pigments responsible for ultraviolet-absorption in nectar guide of flower. *Science*, **177**, 528–530.
- deVetten N, Quattrocchio F, Mol J, Koes R (1997) The *an11* locus controlling flower pigmentation in petunia encodes a novel WD-repeat protein conserved in yeast, plants, and animals. *Genes & Development*, **11**, 1422–1434.
- Vogt T (2010) Phenylpropanoid biosynthesis. *Molecular Plant*, **3**, 2–20.
- Walker AR, Davison PA, Bolognesi-Winfield AC *et al.* (1999) The TRANSPARENT TESTA GLABRA1 locus, which regulates trichome differentiation and anthocyanin biosynthesis in *Arabidopsis*, encodes a WD40 repeat protein. *Plant Cell*, **11**, 1337–1349.
- Wang S, Basten CJ, Zeng Z-B (2007) *Windows QTL Cartographer 2.5* Department of Statistics, North Carolina State University, Raleigh, NC. (<http://statgen.ncsu.edu/qtlcart/WQTLCart.htm>).
- Waser NM, Price MV (1985) The effect of nectar guides on pollinator preference: experimental studies with a montane herb. *Oecologia*, **67**, 121–126.
- Williams PH, Hill CB (1986) Rapid-cycling populations of *Brassica*. *Science*, **232**, 1385–1389.
- Yoshioka Y, Horisaki A, Kobayashi K *et al.* (2005) Intraspecific variation in the ultraviolet colour proportion of flowers in *Brassica rapa* L. *Plant Breeding*, **124**, 551–556.
- Yuan YW, Byers KJRP, Bradshaw HD (2013a) The genetic control of flower-pollinator specificity. *Current Opinion in Plant Biology*, **16**, 422–428.
- Yuan YW, Sagawa JM, Di Stilio VS, Bradshaw HD (2013b) Bulk segregant analysis of an induced floral mutant identifies a MIXTA-like R2R3 MYB controlling nectar guide formation in *Mimulus lewisii*. *Genetics*, **194**, 523–528.
- Yuan YW, Sagawa JM, Frost L, Vela JP, Bradshaw HD (2014) Transcriptional control of floral anthocyanin pigmentation in monkeyflowers (*Mimulus*). *New Phytologist*, **204**, 1013–1027.
- Zhao JJ, Wang XW, Deng B *et al.* (2005) Genetic relationships within *Brassica rapa* as inferred from AFLP fingerprints. *Theoretical and Applied Genetics*, **110**, 1301–1314.

M.T.B and C.W designed the study. M.T.B, L.K.L and M.J.R ran field experiments and collected floral data. N.A.A and C.C performed and analysed biochemical assays. R.J.C.M, M.F.C, U.K.D and J.N.M developed SNP markers and the genetic linkage map. M.T.B and C.W analysed and wrote the study. All authors edited and revised the manuscript.

Data accessibility

Raw input files of floral the UV-pattern survey, floral morphological measurements, biochemical analyses, pollinator observations and genetic linkage map are archived in DRYAD (doi: 10.5061/dryad.cj375).

Appendix 1

Table A1 QTL of petal blade, petal UV region, and floral size and shape traits of *Brassica rapa* RILs raised in the field. Floral traits are listed with associated QTL, chromosome, position (cM), likelihood ratios, per cent variance explained (PVE) by the QTL and additive effect size (a_0) of alleles inherited from R500. Asterisks indicate marginally significant QTL (P -value <0.075). LOD support limits and SNP markers closest to the QTL peaks and support limits are presented in Table S3, Supporting information

QTL	Trait	Chr	Position (cM)	LR	PVE	a_0
QTL1-1	Blade ln	A01	27.8	17.9	6.7	0.013
	UVP	A01	32.7	24.2	8.4	-0.012
	Blade wd	A01	35.6	24.0	8.3	0.017
	Blade ln	A01	39.7	38.2	12.9	0.018
	Blade area	A01	42.5	28.2	12.0	0.012
QTL1-2	Blade area	A01	69.4	14.9 [†]	6.3	0.009
	UV area	A01	77.2	17.7	4.1	0.001
QTL2-1	Blade wd	A02	76.9	14.5 [†]	4.3	-0.012
QTL2-2*	UV ln	A02	108.3	14.9	3.6	-0.004
QTL3-1	Blade area	A03	8.2	16.8	6.9	0.009
QTL3-2	Floral size PC1	A03	28.8	14.4 [†]	4.8	0.242
QTL3-3	UV wd	A03	56.8	14.4 [†]	4.7	-0.009
	UV area	A03	58.8	20.8	4.9	-0.001
	UV ln	A03	58.8	18.7	4.5	-0.005
	UVP	A03	58.8	14.8 [†]	5.0	-0.009
QTL3-4	UV wd	A03	78.5	17.1	5.5	-0.010
QTL3-5	Blade wd	A03	84.2	56.4	22.0	-0.027
	Blade L/W Ratio	A03	84.2	88.4	34.5	0.080
QTL3-6	Blade ln	A03	125.6	22.2	7.2	0.017
QTL3-7	Floral size PC1	A03	131.7	26.4	8.4	0.473
QTL5-1	Blade L/W Ratio	A05	52.6	19.8	4.1	-0.028
	UV area	A05	54.5	15.9	3.7	0.001
	UV ln	A05	57.9	14.5	3.5	0.004
QTL7-1	Blade wd	A07	3.5	18.2	5.3	0.015
	Blade ln	A07	4.5	16.5	5.4	0.012
	Blade area	A07	5.6	21.4	9.3	0.011
	UV L/W Ratio	A07	8.2	16.0	10.6	0.020
QTL7-2	UV wd	A07	25.3	14.7 [†]	4.7	0.007
	UVP	A07	25.7	20.0	6.8	0.011
	UV ln	A07	27.3	46.2	12.3	0.008
	Floral size PC1	A07	27.3	15.9	5.1	0.252
	UV area	A07	27.7	21.1	5.0	0.002
	Blade L/W Ratio	A07	36.0	35.2	9.5	-0.042
	Blade wd	A07	37.6	28.8	10.1	0.018
QTL7-3	UV area	A07	64.0	35.8	9.1	0.002
	UV ln	A07	64.0	33.9	9.5	0.007
	UV wd	A07	64.0	24.8	8.2	0.009
QTL7-4	UVP	A07	71.5	19.2	7.6	0.011
	UV L/W Ratio	A07	76.8	16.9	9.9	0.020
QTL8-1	Blade ln	A08	32.4	14.1 [†]	4.6	0.011
QTL8-2	Blade wd	A08	69.5	30.0	10.6	-0.019
	Blade L/W Ratio	A08	69.5	28.8	7.2	0.037
	UV area	A08	70.8	39.5	9.9	-0.002
	UV ln	A08	70.8	38.0	9.8	-0.007
	UVP	A08	71.6	21.5	7.4	-0.011
QTL9-1	UV wd	A08	72.6	39.8	14.3	-0.012
QTL9-1	Floral size PC1	A09	68.9	53.6	18.8	0.510
QTL9-2	Blade area	A09	100.2	15.5	5.6	0.008
	Blade wd	A09	108.3	17.8	6.5	0.015

Table A1 Continued

QTL	Trait	Chr	Position (cM)	LR	PVE	a_0
QTL9-3	Blade area	A09	130.1	28.1	9.6	0.011
	Floral size PC1	A09	130.9	50.0	17.3	0.462
	Blade ln	A09	131.7	39.7	13.4	0.018
QTL10-1	UV ln	A10	58.9	15.3	3.7	-0.004
	UV ln	A10	67.5	14.6	3.5	-0.004
QTL10-2*	UV area	A10	82.3	28.5	7.0	-0.002
	UV wd	A10	84.0	17.1	5.5	-0.008

*QTL based on LR peak and 1-LOD support limits.

† $P < 0.075$.

Supporting information

Additional supporting information may be found in the online version of this article.

Fig. S1. (A) HPLC separation of methanol extractions from UV-absorbing and UV-reflecting regions of *Brassica rapa* petals raised under field conditions.

Fig. S2. Bivariate scatterplots (below diagonal) and correlation coefficients (above diagonal) of floral size, petal blade, and UV-region traits from *Brassica rapa* RILs raised in the field.

Fig. S3. Clustal omega alignment of *Arabidopsis MYB12* (At2g47460) and a *Brassica rapa* homolog (Bra000453) from R500 and IMB211 accessions.

Fig. S4. Clustal omega alignment of *Arabidopsis* 4-coumarate: CoA ligase 3 (*4CL3*; At1g65060) and a *Brassica rapa* homolog (Bra004109) from R500 and IMB211 accessions.

Table S1. Results of principal components analysis (PCA) of four floral size traits.

Table S2. Detailed information on each *Brassica rapa* sample raised in the field (University of Wyoming, Laramie, WY, USA) or sampled from herbarium sheets (Rocky Mountain Herbarium; University of Wyoming).

Table S3. QTL of petal blade, petal UV-region, and floral size and shape traits of *Brassica rapa* RILs raised in the field. Floral traits are listed with associated QTL, chromosome, QTL peak position and support limits (cM), as well as nearest markers (chromosome and physical location; bp) in the *Brassica rapa* genome v1.1. (for translation of markers from v1.1 to v1.5, see Table S6, Supporting information).

Table S4. *Brassica rapa* genes residing between 1LOD and 2LOD support limits of QTL3-3.

Table S5. *Brassica rapa* genes residing between 1LOD and 2LOD support limits of QTL7-3.

Table S6. SNP markers used in the *Brassica rapa* linkage map and their chromosome and position (bp) in the *Brassica rapa* genome v1.1 and v1.5.

Data S1. Linkage map construction.